ISSN 2176-5480

22nd International Congress of Mechanical Engineering (COBEM 2013)
November 3-7, 2013, Ribeirão Preto, SP, Brazil

CIRCUITRY DESIGN OF POLYMER PLATE HEAT EXCHANGERS BASED ON ENTROPY GENERATION MINIMIZATION

Mariana T. Tamura
Jader R. Barbosa Jr.
POLO - Research Laboratories for Emerging Technologies in Cooling and Thermophysics, Department of Mechanical Engineering, Federal University of Santa Catarina, Florianópolis, SC, 88040-900, Brazil
E-mail: jrb@polo.ufsc.br

Abstract. *Recent developments on polymers and polymer matrix composites have allowed significant improvements in their thermal and mechanical properties, enabling their application as construction materials for heat exchangers. Although the thermal conductivities of polymer composites are still significantly lower than those of metals, advantage can be taken of their favorable mechanical properties and low cost to develop new types of heat exchangers. The purpose of this paper is to develop a procedure to evaluate the effectiveness of a given refrigerant circuit geometry in a plate heat exchanger. For a specified heat transfer rate and temperature span, the optimum channel diameter can be calculated based on the minimization of the entropy generation due to heat transfer and pressure drop. The effectiveness of a given refrigerant circuit is quantified in terms of a figure of merit defined as the ratio of the overall surface efficiency and the product of the circuit volume and refrigerant pumping power. The analysis is exemplified with a comparison of the results of the figure of merit for three possible refrigerant circuits of a rectangular polymer plate heat exchanger intended for personal cooling applications.*

Keywords: *Polymer heat exchangers, plate heat exchanger, circuit design, entropy generation minimization, heat transfer.*

1. INTRODUCTION

Although metallic heat exchangers are used extensively due to their superior thermal performance, their use is not so advantageous in some applications involving weight restrictions or chemical compatibility issues (e.g., fouling and chemical reactions). Among the many advantages of thermally conductive plastics and polymer composites are: (i) reduced weight (low density), (ii) low cost, (iii) compatibility with some corrosive fluids, (iv) lower coefficients of thermal expansion, (v) architectural flexibility and (vi) integrated manufacturing (i.e., elimination of costly post-machining operations). Nevertheless, plastics have thermal conductivities typically 2 or 3 times lower than those of metallic materials, which is one of the greatest barriers against a more widespread use of polymers in heat exchangers.

Applications of polymeric materials in heat exchangers have been reviewed by several authors (Zaheed and Jachuck, 2004; Malik and Bullard, 2005; Bar-Cohen *et al.*, 2008; T'Joen *et al.*, 2009). Zaheed and Jachuck (2004) reviewed the properties of polymers emphasizing the development and utilization of thin polymer film heat exchangers. The use of thin polymer films is recommended, as opposed to polymer plates and tubes, in order to compensate for the low thermal conductivity of the polymer material. Basic heat transfer calculations considering the thermal properties of PVDF (polyvinylidene fluoride) and Hastelloy (a Ni-Cr-Mo alloy) have shown that, although the surface area of a polymer heat exchanger was six times larger than that of the metallic counterpart, a tube bundle of Ni-Cr-Mo alloy would cost 2.5 times as much as a PVDF bundle. Malik and Bullard (2005) pointed out potential applications of polymer heat exchangers in HVAC&R, such as skin condensers for household refrigerators and compact tube bundles as indirect expansion evaporators and condensers for stationary and mobile air conditioning (A/C) units. Calculations showed that a hypothetical 1-ton A/C system equipped with optimally-configured polymer heat exchangers had a thermal performance similar to a conventional system, but the volume occupied by the polymer heat exchangers was 20 times larger due to the absence of extended surfaces. Bar-Cohen *et al.* (2008) presented a review of the properties and characteristics of commercially-available thermally-conductive polymers. A thermal-hydraulic model of a doubly-finned plate heat exchanger for seawater-cooled applications (with a 20 W/m.K thermoplastic) was shown to achieve nearly half the heat transfer rate of an aluminum heat exchanger at the same operating conditions, and 80% of the heat transfer rate of a corrosion-resistant metallic heat exchanger. T'Joen *et al.* (2009) reviewed the use of polymers in heat exchangers in HVAC&R and considered them as promising materials, specially in the context of the recent advances in composite materials and nanoscale composites.

Lee *et al.* (2011) conducted a study on the applicability of polymer heat exchangers as evaporators in an automatic defrost bottom-mount 280-liter refrigerator/freezer. Evaporators made of PBT (polybutylene terephthalate) and PTFE (polytetrafluorethylene) carbon composites were evaluated in refrigerator pull-down tests, giving similar cooling capacities to those of a metal fin-tube evaporator. The geometry of plastic evaporator used by Lee *et al.* (2011) has not been disclosed. Separate tests were conducted to evaluate the frosting behavior on the plastic prototypes, which was seen to be influenced by the thermal conductivity and surface characteristics (contact angle) of the material. The frost thickness and surface heat and mass transfer characteristics was quite similar for the aluminum and PBT substrates due to higher thermal

ISSN 2176-5480

conductivity of the latter (1.5 W/m.K) compared to those of the other polymer substrates (0.24, 0.47 and 0.72 W/m.K). The contact angle of the PBT surface was 82°, while that of the aluminum and PTFE surfaces were 82° and ∼ 96°, respectively. Hesse and Weimer (2012) discussed the applications of polymer film heat exchangers for liquid-liquid and gas-liquid processes in a number of refrigeration applications with and without phase change at pressures below 5 bar.

Despite the increasing number of studies, little has been discussed on the optimal configuration of the liquid channels in gas-liquid polymer plate heat exchangers. In this paper, we present a procedure to design polymer plate heat exchangers in which the internal fluid flow channel is optimized for minimum entropy generation and the best channel configuration in the plate (flow circuit) is determined based on the value of a heat exchanger figure of merit involving the overall surface efficiency, internal fluid volume and fluid pumping power. Three different configurations have been evaluated based on their performance, with the best result presented by a parallel channel arrangement.

2. MODELING

2.1 Determination of the channel geometry

2.1.1 Heat transfer

A structurally flexible plate heat exchanger is to be designed for a specified thermal duty using a high thermal conductivity polymer composite. In the present study, the thermal properties of reinforced polyurethane — with typical values of thermal conductivity between 1.2 and 4.0 W/m.K (Ovation Polymers Technology, 2012) — have been adopted as a reference. The working fluid is a liquid (aqueous solution) that flows through channels fabricated in the plate (by, say, machining, die-stamping or roll-bonding). In this study, properties of water have been adopted. The external fluid is air, with specified values of heat transfer coefficient and free-stream temperature.

As polymers have much lower thermal conductivities than metals, for a given heat exchanger surface area, the channel length must be much larger than in a metal plate heat exchanger in order to compensate for the lower surface efficiency. As the pressure drop in the channel is directly proportional to its length, the fluid flow circuit has to be optimized to give the best relationship between heat transfer and pumping power.

In the present analysis, the total heat transfer rate (thermal load) is specified as well as the temperature range of the working fluid. Thus, an energy balance on the fluid stream gives the fluid flow rate as follows:

$$\dot{m} = \frac{q}{c_p \left(T_{out} - T_{in}\right)} \tag{1}$$

where $(T_{out} - T_{in})$ is the temperature range and q is the heat transfer rate calculated from the log-mean temperature difference relationship given by:

$$q = UA\Delta T_{LM} = UA\frac{\Delta T_{out} - \Delta T_{in}}{\ln\left(\Delta T_{out}/\Delta T_{in}\right)} \tag{2}$$

where $\Delta T_{in} = T_\infty - T_{in}$ and $\Delta T_{out} = T_\infty - T_{out}$.

It is hypothesized that the unit cell of the plate heat exchanger consists of a fluid channel with two external fins, as shown in Fig. 1. Taking the internal channel area as a reference, the total length of the channel is given by:

$$L = \frac{q}{\pi d_i U \Delta T_{LM}} \tag{3}$$

where the overall heat transfer coefficient based on the internal area is defined as:

$$\frac{1}{U} = \frac{1}{h_i} + \frac{\ln\left(d_o/d_i\right)d_i}{2k_w} + \frac{1}{\eta_o h_o}\left(\frac{\pi d_i}{4L_f + \pi d_o - 4e}\right) \tag{4}$$

where the term in parenthesis on the right is the ratio of the internal and external surface areas, and L_f and e are the fin length and half thickness, respectively. The overall surface efficiency is defined as (Lienhard and Lienhard, 2001):

$$\eta_o = 1 - (1 - \eta_f)\frac{A_f}{A_o} = 1 - (1 - \eta_f)\left(\frac{4L_f}{4L_f + \pi d_o - 4e}\right) \tag{5}$$

where the efficiency of a rectangular fin with a thermally insulated tip is calculated from:

ISSN 2176-5480

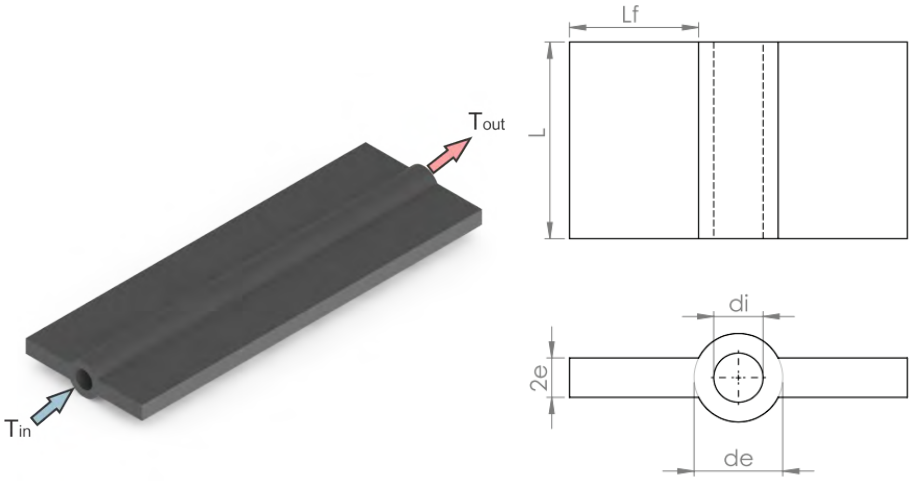

(a) Schematic view. (b) Basic dimensions.

Figure 1: Elementary unit cell of the plate heat exchanger (circular channel shown for simplicity).

$$\eta_f = \frac{\tanh(mL_f)}{mL_f} \tag{6}$$

where:

$$m = \left(\frac{h_o P_f}{k_w A_{c,f}}\right)^{1/2} = \left(\frac{h_o}{k_w e}\right)^{1/2} \tag{7}$$

In order to operate as close as possible to optimum thermal conditions with approximately 95% of the fin heat transfer rate taking place in the first $2/m$-long segment of the fin, the fin length has been specified as (Lienhard and Lienhard, 2001):

$$L_f = \frac{2}{m} = 2\left(\frac{k_w e}{h_o}\right)^{1/2} \tag{8}$$

2.1.2 Entropy generation minimization

The internal diameter d_i is calculated via the entropy generation minimization method proposed by Bejan (1995a). In channel flows, the rate of entropy generation per unit channel length is given by:

$$\dot{S}'_{gen} = \dot{S}'_{gen,\Delta T} + \dot{S}'_{gen,\Delta p} = \frac{q'\Delta T}{T^2} + \frac{\dot{m}}{\rho T}\left(-\frac{dp}{dx}\right) \tag{9}$$

where the first term on the right is the rate of entropy generation due to heat transfer with a finite temperature difference and the second term is the entropy generation rate due to friction. Equation (9) can be written in terms of the friction factor, f, and the Nusselt number, Nu_{d_i}, defined by:

$$f = f(Re_{d_i}) = \frac{\rho d_i}{2G^2}\left(-\frac{dp}{dx}\right) \tag{10}$$

$$Nu_{d_i} = f(Re_{d_i}, Pr) = \frac{q'}{P\Delta T}\frac{d_i}{k} \tag{11}$$

Thus:

ISSN 2176-5480

$$\dot{S}'_{gen} = \frac{q'}{\pi k T^2 N u_{d_i}} + \frac{32\dot{m}^3}{\pi^2 \rho^2 T} \frac{f}{d_i^5} \tag{12}$$

where T is the bulk stream fluid temperature and the f and Nu_{d_i} are functions of the channel diameter through the Reynolds number defined as:

$$Re_{d_i} = \frac{4\dot{m}}{\pi \mu d_i} \tag{13}$$

The entropy generation number is the dimensionless entropy generation rate given by:

$$N_s = \frac{\dot{S}_{gen}}{\dot{m} c_p} \tag{14}$$

2.2 Determination of the best fluid flow circuit

2.2.1 Figure of merit

In the design of the polymer plate heat exchanger, the optimal flow circuit configuration is one which allows a uniform temperature distribution on the external surface while consuming the least amount of power to maintain this condition. Therefore, the following figure of merit is proposed as an objective function to identify the most suitable fluid flow circuit:

$$\phi = \frac{\eta_o}{W_p V_i} \tag{15}$$

The objective function, ϕ, is maximum for a flow circuit configuration which has an overall surface efficiency, η_o, close to unity and the lowest fluid pumping power through the channels, W_p. V_i is the volume of the fluid channels, which should be as small as possible to reduce the weight of the heat exchanger. This is of particular significance in portable applications. However, it should be noted that a small value of V_i is not a guarantee of a good or optimum heat exchanger, as a poorly designed circuit with a small value of V_i would result in a small value of η_o because of the low thermal conductivity of the polymeric material.

In what follows, the performance of three different fluid flow circuits is evaluated from the point of view of their figure of merit. In all of them, the channel diameter is determined via the minimization of entropy generation method described above.

2.2.2 Configuration 1: Coiled single channnel

This configuration consists of a single channel for which it is possible to find the size of the square plate as a function of the number of coil passes, according to Fig. 2.

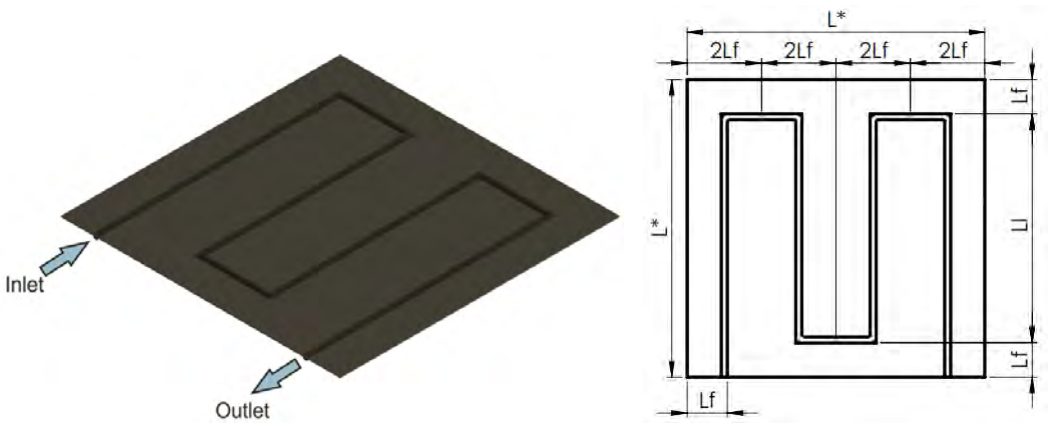

(a) Schematic view. (b) Basic dimensions.

Figure 2: The coiled single channel plate heat exchanger.

ISSN 2176-5480

Defining L^* as the side of the square and L_l as the length of the section between bends, the area of one side of the square plate A_{sq} is given by:

$$A_{sq} = {L^*}^2 \tag{16}$$

where two definifitions of L^* are possible:

$$L^* = 2L_f + L_l \tag{17}$$

and:

$$L^* = 2n(L_f + d_o/2) \tag{18}$$

Since $d_o \ll L_f$, then $L_f + d_o/2 \approx L_f$, and combining Eqs. (17) and (18) gives:

$$2L_f + L_l = 2nL_f \tag{19}$$

As shown in Fig. 3, it is possible to write the total channel length, L, as the combination of n elementary segments (units) of identical unit length $(2L_f + L_l)$. Thus,

$$L = n(2L_f + L_l) \tag{20}$$

or:

$$\frac{L}{n} = 2nL_f \tag{21}$$

Rearranging Eq. (21), the minimum number of passes needed to obtain a total channel length L that satisfied the design constraints is given by:

$$n = \sqrt{\frac{L}{2L_f}} \tag{22}$$

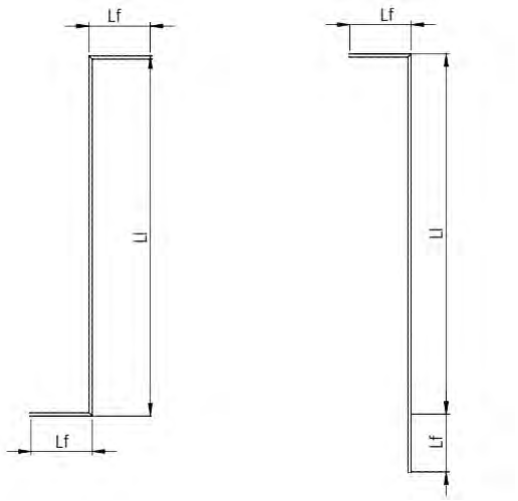

(a) Intermediate unit cell. (b) End unit cell.

Figure 3: The unit cells of the coiled single channel plate heat exchanger.

Since the right-hand side of Eq. (22) is not necessarily a whole number, the number of passes is the integer immediately below or above the resulting real number. If the smaller integer is selected, the heat exchanger dimensions are smaller, but the heat duty is not satisfied. On the other hand, the higher number is a conservative option, as the nominal heat duty is guaranteed at the expense of a slightly larger heat exchanger. Therefore, the design value of n is taken as the integer number immediately above the result of Eq. (22).

ISSN 2176-5480

2.2.3 Configuration 2: Nested single channnel

This configuration consists of a single channel in a nested arrangement, as shown in Fig. 4. Here, an additional length of size $3x$ is needed on the sides of the square heat exchanger in order to complete the total channel length and compensate for the fin length, L_f, being used as a minimum half-spacing between adjacent channels. The value of x can be computed from Fig. 4(b) as follows:

$$x = \frac{L - 32L_f}{22} \tag{23}$$

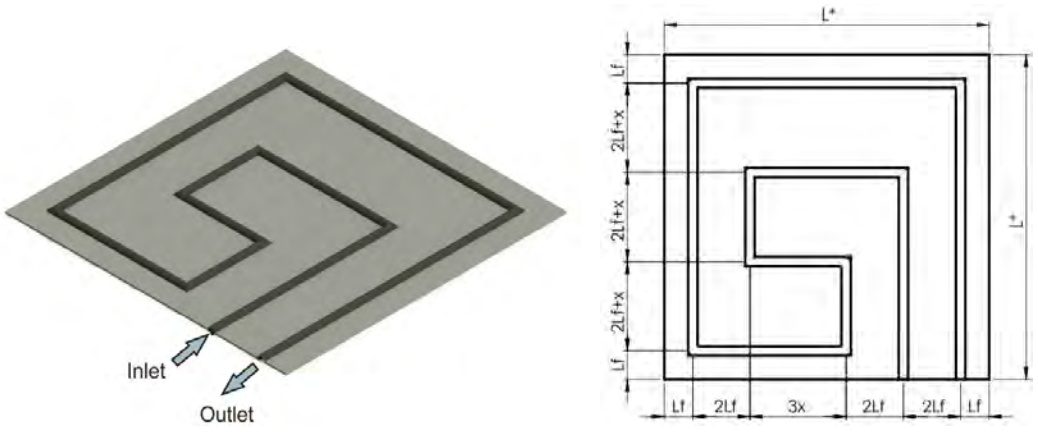

(a) Schematic view. (b) Basic dimensions.

Figure 4: The nested single channel plate heat exchanger.

In the coiled and nested single channel geometries, the pumping power is calculated based on the combination of distributed head losses in the straight tube segments and minor head losses in 90° elbows. Thus:

$$W_p = \dot{m} g \left(h_f + h_D\right) = \dot{m} \left(f \frac{L}{d_i} + N K_L\right) \tag{24}$$

where N is the number of 90° elbows in the circuit and $K_L = 1.1$ is the associated loss coefficient (Çengel and Cimbala, 2006).

2.2.4 Configuration 3: Parallel channnels

In this configuration, q is assumed to be divided equally into parallel channels in order to investigate the existence of an optimum number of channels that maximizes the figure of merit. The number of parallel channels that gives the most compact geometry (i.e., the one with the greatest area per unit perimeter) can also be computed.

In order to simplify the analysis, the following hypothesis are made regarding the parallel channel configuration: (i) heat transfer in the inlet and outlet manifolds is negligible; (ii) the total mass flow rate is equally distributed between the n parallel channels; (iii) the cross-section area of the manifolds is constant and uniform; (iv) minor losses in the manifold junctions are calculated using loss coefficients for single-phase flow in tee junctions (Çengel and Cimbala, 2006). The heat transfer rate per channel is defined as:

$$q_n = \frac{q}{n} \tag{25}$$

The diameter of the inlet and outlet manifolds was determined based on the fact that, for a given mass flow rate, the pressure drop in a pipe section is inversely proportional to the pipe diameter. Thus, for a specified average manifold Reynolds number, $Re_{D,M}$, the manifold diameter is calculated from:

$$D = \frac{4\dot{m}_M}{Re_{D,M} \pi \mu} \tag{26}$$

where the average mass flow rate in the manifolds is defined as:

ISSN 2176-5480

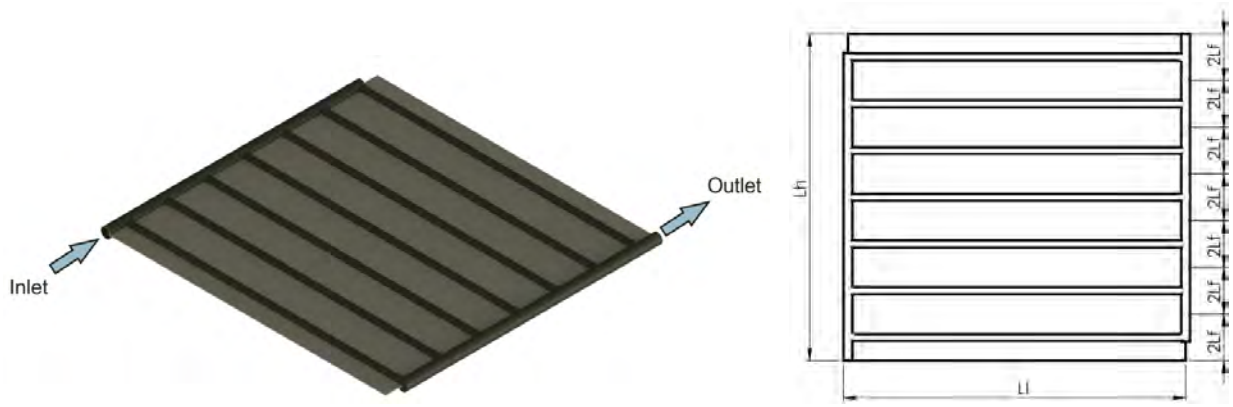

(a) Schematic view. (b) Basic dimensions.

Figure 5: The parallel-channel plate heat exchanger.

$$\dot{m}_M = \frac{\dot{m} + \dot{m}_n}{2} \tag{27}$$

and $\dot{m}_n$ is the mass flow rate per channel. It should be noted that a fixed value of 250 was assigned to $Re_{D,M}$ in order to avoid excessivelly large values of the manifold diameter D.

As mentioned above, the configuration that gives the most compact geometry has been computed. In this case, in order to have the greatest area per unit perimeter, the length of the channels should be equal to the sum of the fin lengths of each channel. Thus:

$$L_l \approx 2nL_f \tag{28}$$

which means that $|L_l - 2nL_f|$ should be as small as possible.

2.3 Conditions and implementation

Table 1 summarizes the baseline parameters and conditions adopted in the simulations. The working fluid is water and the external fluid is air. The mathematical models presented in this section were implemented in Matlab.

Table 1: Baseline conditions and parameters of the simulations

Heat transfer rate	100 W
Inlet temperature (water)	293 K
Outlet temperature (water)	298 K
Temperature range (water)	5 K
Thermal conductivity of the polymeric material	4 W/mK
Wall thickness	3 mm
External heat transfer coefficient	5 W/m^{2}K
Free-stream temperature of the air	310 K

3. RESULTS

Results are initially presented for the entropy generation minimization in the straight-channel heat exchanger (no minor losses) in order to evaluate the influence of the geometric and physical parameters. Next, the different channel configurations are evaluated in the light of the proposed figure of merit, ϕ.

3.1 Comparison between different cross-section geometries

The mathematical model presented in Section 2 was employed to determine the channel cross-section geometry that resulted in the minimal entropy generation rate in the straight-channel heat exchanger. Figure 6 demonstrates the existence

ISSN 2176-5480

of a circular channel diameter that minimizes the entropy generation number resulting from a combination of entropy generation due to fluid friction and heat transfer with a finite temperature difference (Bejan, 1995b). On the left of the minimum, the entropy generation number is higher than the minimum because of the dependence of the entropy generation rate due to friction with the inverse of the fifth power of the channel diameter (see Eq. 12). On the right of the minimum, the entropy generation number due to heat transfer is larger due to the reduction of the heat transfer coefficient with the channel diameter, which results in an increase of the wall temperature in order to satisfy the constant thermal load (heat transfer rate).

For the conditions reported in Fig. 6, it was observed that the point of minimum corresponds to a value of Reynolds number less than 1000, which is in agreement with conclusions from previous works (Zaheed and Jachuck, 2004) where it has been suggested that laminar flows are strongly reccommended in applications where the pressure drop is an important design constraint.

The effect of channel geometry is illustrated in Fig. 7, which shows the behavior of N_s as a function of the channel aspect ratio for the triangular, rectangular and ellipsoidal geometries. Operating conditions are those shown in Table 1. The relationships of Shah and Bhatti (1987) for the friction factor and Nusselt number in fully developed laminar flow with constant wall temperature for the circular, rectangular, ellipsoidal and triangular channels as a function of the cross-section aspect ratio were used in the calculation of the entropy generation number. Table 2 shows the minimum values of entropy generation number for the three geometries. As can be seen, the triangular cross-section yields the lowest value of entropy generation number with the longest channel. However, it can be concluded that this advantage in terms of thermal performance may be not enough to compensate for the additional complexity in manufacturing associated with the triangular cross-section. Thus, in the remainder of this paper, the circular cross-section (ellipse with an aspect ratio equal to unity) will be considered.

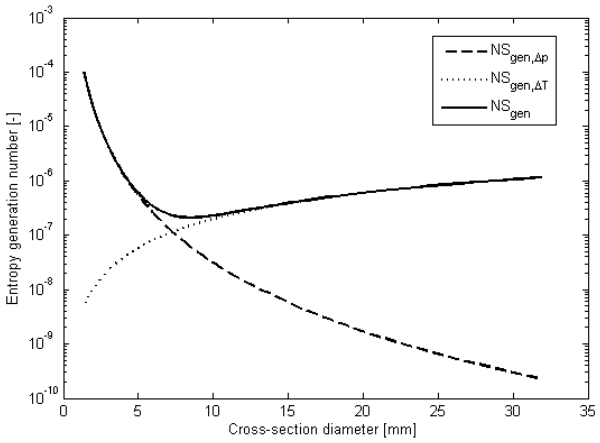

Figure 6: Effect of the circular channel diameter on the entropy generation number.

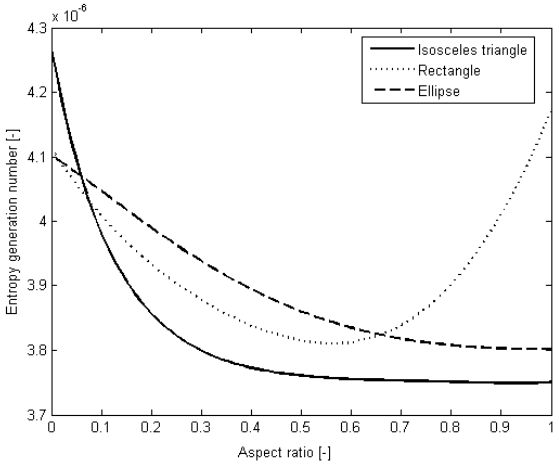

Figure 7: Behavior of N_S as a function of the channel aspect ratio for the various channel geometries.

Table 2: Comparison between the best channel aspect ratio for the various channel geometries.

Geometry	Isosceles triangle	Rectangle	Ellipse
Entropy generation number	4.91×10^{-6}	5.09×10^{-6}	5.12×10^{-6}
Cross-section aspect ratio	0.33	0.60	1.00
Length [m]	8.77	8.16	8.00
Hydraulic diameter [m]	5.0×10^{-3}	5.1×10^{-3}	5.1×10^{-3}
Reynolds number	1266	1243	1239

3.2 Influence of the polymer thermal conductivity

As can be seen from Fig. 8, there is an asymptotic decrease of the minimum N_S with respect to the thermal conductivity of the heat exchanger material. This is because higher thermal conductivities give rise to smaller temperature differences between the internal and external surfaces of the plate heat exchanger, which result in smaller entropy transfer rates. Moreover, the increase in thermal conductivity implies that the optimal configurations will present progressively smaller values of Re_{d_i}, thus yielding larger values of the optimal d_i as k_w increases. It is also worthy of note that the

ISSN 2176-5480

increase in optimal diameter is very small for the range of conditions evaluated: for $k_w = 0.5 - 10$ W/(mK), the optimal diameter increases by only 1.4 mm.

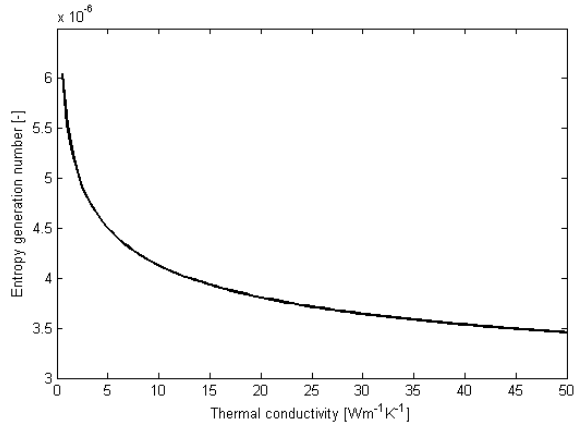

Figure 8: Influence of thermal conductivity on the minimum N_S.

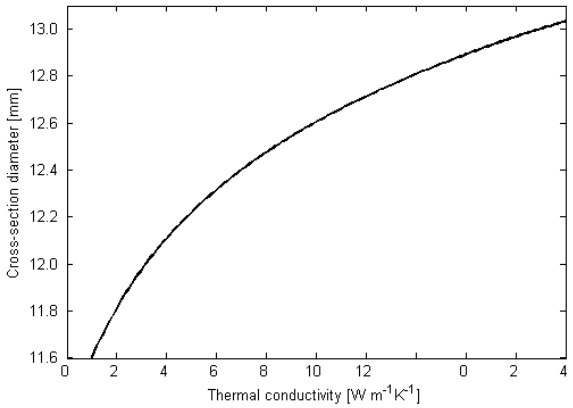

Figure 9: Influence of thermal conductivity on the channel diameter.

The influence of the thermal conductivity of the plate on the spacing between channels (i.e., the fin length in Eq. 8) and on the channel length is shown in Figs. 10 and 11, respectively. Opposite to what has been found for the channel diameter, k_w is seen to strongly influence both variables, which makes clear that the thermal conductivity has a crucial role in the figure of merit defined in Eq. (15) since a reduction in the channel length and an increase in the fin length contribute to a reduction of the internal volume of the heat exchanger for a fixed thermal load.

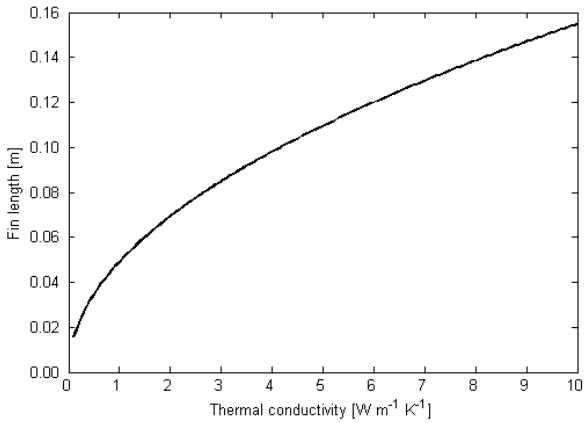

Figure 10: Influence of thermal conductivity on the half-spacing between channels.

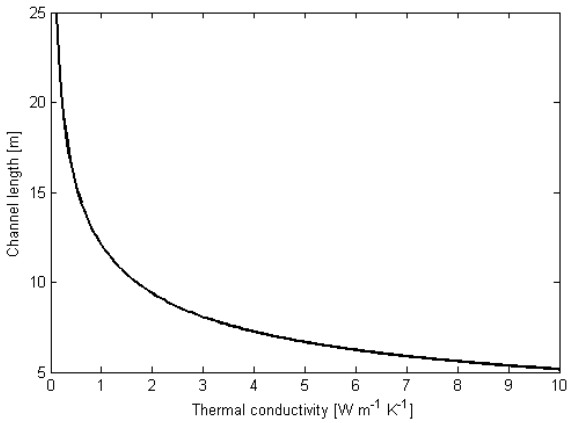

Figure 11: Influence of thermal conductivity on the channel length.

3.3 Effect of the thermal load

The influence of the applied thermal load on the heat exchanger parameters are investigated while keeping the remaining conditions as shown in Table 1. As can be seen in Fig. 12, the point of minimum entropy generation is shifted to larger values of Re_{d_i} as the thermal load is increased from 50 to 150 W at the same time as the minimum N_S increases slightly. It can be inferred from this behavior that to compensate for the increase in entropy generation due to heat transfer the Reynolds number increases, thus resulting in a lower friction factor and a smaller contribution due to friction in the total entropy generation rate.

Although the thermal load (heat transfer rate) does not alter significantly the optimal diameter (Fig. 13), it obviously has a much stronger effect on the channel length, as can be seen from Fig. 14. The pumping power, on the other hand, remains pratically the same for thermal loads between 50 and 150 W for $Re_{d_i} \leq 1000$ (Fig. 15). Table 3 presents a summary of the heat exchanger parameters associated with the conditions of minimum entropy generation number for each applied thermal load.

ISSN 2176-5480

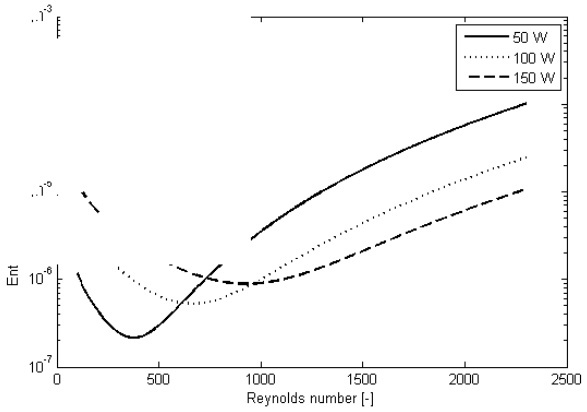

Figure 12: Influence of the thermal load on N_S: Variation of the minimum Re_D.

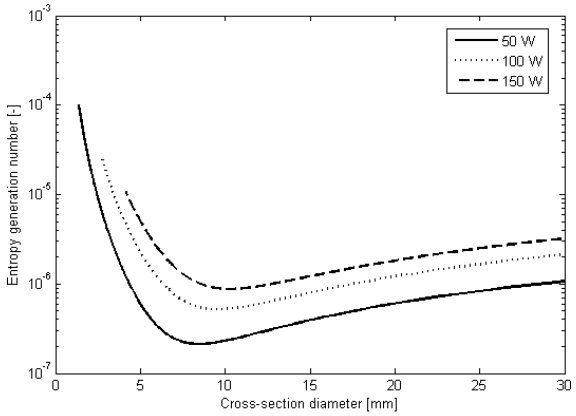

Figure 13: Influence of the thermal load on N_S: Variation of the optimal D_i.

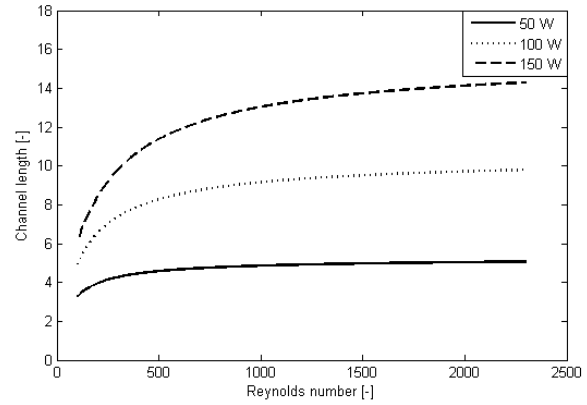

Figure 14: Influence of the thermal load on the heat exchanger length.

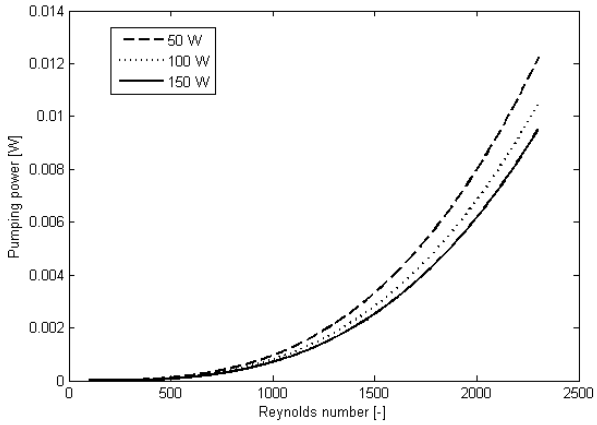

Figure 15: Influence of the thermal load on the pumping power.

Table 3: Comparison of the heat exchanger parameters at the conditions of minimum entropy generation as a function of the thermal load.

Thermal load [W]	50	100	150
Minimum entropy generation number [-]	2.15×10^{-7}	5.27×10^{-7}	8.89×10^{-7}
Optimum diameter [mm]	8.5	9.6	10.3
Channel length [m]	4.42	8.69	12.89
Pumping power [mW]	4.65×10^{-2}	2.26×10^{-1}	5.70×10^{-1}
Reynolds number [-]	375	666	932

3.4 Analysis of the heat exchanger configurations

This section presents an analysis of the three plate heat exchanger configurations based on the figure of merit, ϕ. As mentioned before, the simulation conditions are those presented in Table 1. The results for Configurations 1 (coiled arrangement) and 2 (nested arrangement) are shown in Tables 4 and 5, respectively. Despite the larger internal volume, the nested configuration exhibits a larger figure of merit, thus representing a better plate design.

As far as configuration 3 is concerned, two different criteria were chosen to identify the best number of parallel channels: the figure of merit, ϕ, or the most compact arrangement, i.e., the configuration that yields a square plate geometry.

The number of parallel channels was varied from 1 to 50 in order to identifiy the existence of a point of maximum figure of merit. The behavior of the minimum entropy generation number and of the figure of merit as a function of the number of channels is shown in Figs. 16 and Fig. 17, respectively. The minimum N_S behavior is asymptotic and seen to vary very little for a number of channels greater than 10. In other words, there is little benefit in increasing the number of channels as the product of the sides of the heat exchanger varies only between 1.40 and 1.50 m^2 over the interval.

ISSN 2176-5480

Table 4: Results for Configuration 1 (coiled).

D_h [mm]	9.76
L^* [m]	1.37
h_t [mm]	7.68
V_i [m^3]	3.572 $\times 10^{-4}$
W_p [mW]	0.357
ϕ [W^{-1}m^{-3}]	1.978 $\times 10^{6}$

Table 5: Results for Configuration 2 (nested).

D_h [mm]	9.76
L^* [m]	1.32
h_t [mm]	5.69
V_i [m^3]	5.606 $\times 10^{-4}$
W_p [mW]	0.265
ϕ [W^{-1}m^{-3}]	3.418 $\times 10^{6}$

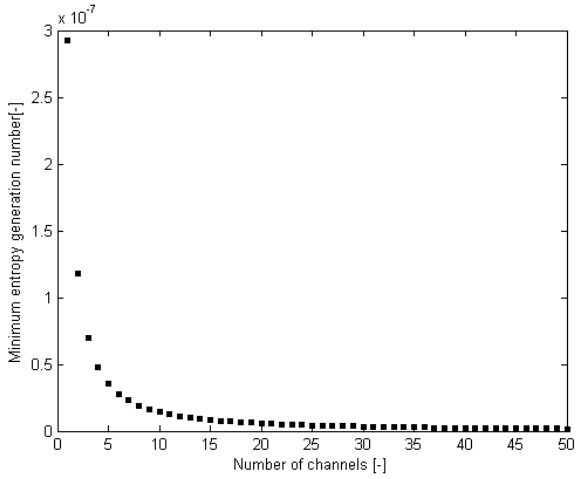

Figure 16: Minimum N_S as a function of the number of parallel channels.

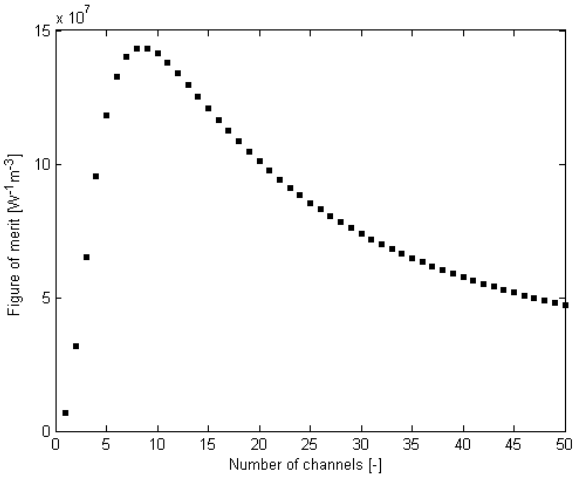

Figure 17: Figure of merit as a function of the number of parallel channels.

Figure 17 demonstrates the existence of an optimal value of ϕ, which corresponds to a heat exchanger with 8 parallel channels. This point of maximum ϕ results from the occurrence of a minimum V_i (Fig. 18), with W_p decreasing continuously (Fig. 19) as η_o remains virtually constant. According to the criterion for the most compact arrangement, a plate heat exchanger with 8 channels also has the best performance due the smallest difference between the sides of the plate, L^* and L_l, as can be seen from Table 6.

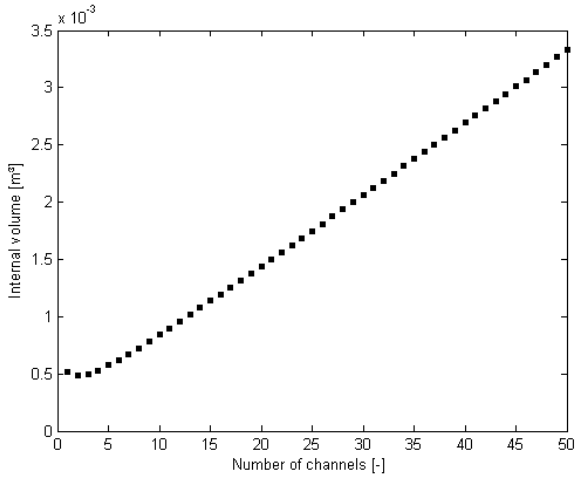

Figure 18: Internal volume as a function of the number of parallel channels.

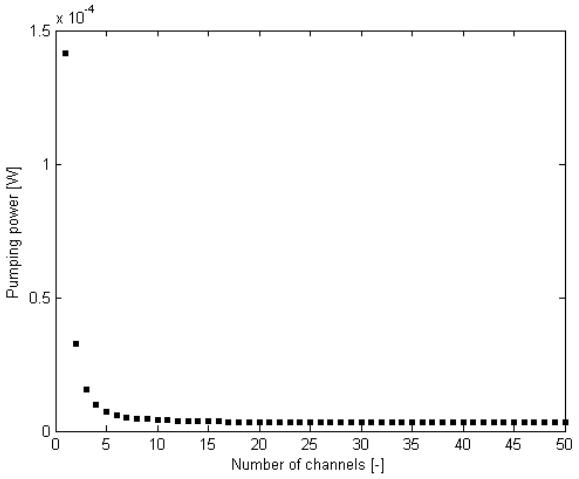

Figure 19: Pumping power as a function of the number of parallel channels.

4. CONCLUSIONS

This paper advanced a calculation procedure for sizing polymer plate heat exchangers based on the minimization of the entropy generation due to finite-temperature difference heat transfer and pressure drop. This procedure has been combined with a selection criterion based on a figure of merit defined as the ratio of the overall surface efficiency and the product of

ISSN 2176-5480

Table 6: Summary of the results for Configuration 3.

Number of channels	2	8	12	50
D_h [mm]	8.47	6.64	6.17	4.90
L^* [m]	0.32	1.28	1.92	8.00
L_l [m]	4.42	1.14	0.77	0.19
h_t [mm]	2.23	0.896	0.983	2.96
V_i [m^3]	5.59×10^{-4}	6.21×10^{-4}	7.44×10^{-4}	2.19×10^{-3}
W_p [W]	5.19×10^{-5}	5.21×10^{-6}	3.81×10^{-6}	2.75×10^{-6}
ϕ [W^{-1}m^{-3}]	1.76×10^{7}	1.55×10^{8}	1.76×10^{8}	8.17×10^{7}

the circuit volume and refrigerant pumping power. A parametric analysis has explored the influence of the polymer thermal conductivity, channel cross-section area and thermal load on the entropy generation number. The analysis combined with the figure of merit was applied in the comparison of three possible refrigerant circuits of a rectangular polymer plate heat exchanger intended for personal cooling applications. The best results were found for the parallel channel configuration, followed by the nested single channel and the coiled channel configurations.

5. ACKNOWLEDGEMENTS

The authors thank the CNPq for financial support through grant No. 573581/2008-8 (National Institute of Science and Technology in Cooling and Thermophysics).

6. REFERENCES

Bar-Cohen, A., Rodgers, P. and Cevallos, J.G., 2008. "Application of thermally enhanced thermoplastics to seawater-cooled liquid-liquid heat exchangers". In *5th European Thermal-Sciences Conference*. , The Netherlands, 2008.

Bejan, A., 1995a. "Entropy generation minimization: the new thermodynamics of finite-size devices and finite-time processes". *Journal of Applied Physics*, Vol. 79, pp. 1191–1218.

Bejan, A., 1995b. *Entropy Generation Minimization*, CRC Press.

Çengel, Y.A. and Cimbala, J.M., 2006. *Fluid Mechanics*. McGraw-Hill.

Hesse, U. and Weimer, T., 2012. "Polymer material heat exchangers application in refrigerant cycles". In *Proc. of the International Refrigeration and Air Conditioning Conference at Purdue*. West Lafayette, p. Paper 2156.

Lee, J., Lee, M. and Jeon, S., 2011. "A study of plastic evaporator for domestic freezer/refrigerator". In *Proceedings of the 23rd International Congress of Refrigeration*. Prague, Czech Republic, p. Paper 163.

Lienhard, J.H. and Lienhard, J.H., 2001. *A Heat Transfer Textbook*. Phlogiston Press, 3rd edition.

Malik, T. and Bullard, C.W., 2005. "Suitability of polymer heat exchangers for air conditioning applications".

Ovation Polymers Technology, 2012. "Nemcon H Product Data Sheet". URL `http://www.opteminc.com/`.

Shah, R.K. and Bhatti, M.S., 1987. *Handbook of Single-Phase Convective Heat Transfer*, Wiley, chapter 3.

T'Joen, C., Park, Y., Wang, Q., Sommers, A., Han, X. and Jacobi, A., 2009. "A review on polymer heat exchangers for HVAC & R applications". *International Journal of Refrigeration*, Vol. 32, pp. 763–779.

Zaheed, L. and Jachuck, R., 2004. "Review of polymer compact heat exchangers, with special emphasis on a polymer film unit". *Applied Thermal Engineering*, Vol. 24, pp. 2323–2358.

7. RESPONSIBILITY NOTICE

The authors are the only responsible for the printed material included in this paper.